



Accepted Article

Title: Self-delivery nanoparticles of amphiphilic acyclic enediynes for efficient tumor cell suppression

Authors: Jing Li, Yuequn Wu, Lili Sun, Shuai Huang, Baojun Li, Yun Ding, Aiguo Hu*

This manuscript has been accepted and appears as an Accepted Article online.

This work may now be cited as: *Chin. J. Chem.* **2019**, *37*, 10.1002/cjoc.201900034.

The final Version of Record (VoR) of it with formal page numbers will soon be published online in Early View: <http://dx.doi.org/10.1002/cjoc.201900034>.

Self-delivery nanoparticles of amphiphilic acyclic enediynes for efficient tumor cell suppression

Jing Li^a, Yuequn Wu^b, Lili Sun^b, Shuai Huang^a, Baojun Li^a, Yun Ding^a, Aiguo Hu^{*a}

^a Shanghai Key Laboratory of Advanced Polymeric Materials, School of Materials Science and Engineering, East China University of Science and Technology, Shanghai 200237, China

^b The State Key Laboratory of Bioreactor Engineering, East China University of Science and Technology, Shanghai, 200237, China

Cite this paper: *Chin. J. Chem.* 2019, 37, XXX–XXX. DOI: 10.1002/cjoc.201900XXX

Four acyclic maleimide-based enediyne compounds with different hydrophilicity were synthesized through Sonogashira reaction to reveal a self-delivery antitumor drug platform. As proved by ESR analysis, the enediyne compounds undergo Bergman-like cyclization and generate diradical intermediates at physiological temperature, which are able to induce DNA-cleavage through the abstraction of H atoms from the sugar-phosphate backbones. When the critical aggregation concentration is reached in water, the amphiphilic enediyne compounds self-assemble into nanoparticles and possess the self-delivery ability to be facily admitted by tumor cells, resulted in greatly improved cytotoxicity (IC₅₀ down to 10 μM) and much higher tumor cell apoptosis rate (up to 86.6%) in comparison with either the hydrophilic or the lipophilic enediyne compound. The enhanced endocytosis of the amphiphilic enediyne compounds was further confirmed through confocal laser scanning microscopy analysis. The unveiled relationship between the hydrophilicity of enediyne drugs and their therapeutic efficacy will provide a guideline for the design of new self-delivery drugs employed in medicinal applications.

Introduction

Cancer is a complex disease causing severe pain on the patients and ranked as the leading cause of human death. Cancer is considered as the single most important barrier to increasing life expectancy in all the countries in the 21st century according to the GLOBOCAN results in 2018.¹ In recent years, various therapeutics have been developed for cancer treatment including chemotherapy, immunotherapy, radiation therapy and surgical excision^{2,3}. Among these therapeutics, the chemotherapy, which relies on the high cytotoxicity of chemotherapeutic agents plays an important role. It is therefore critical to explore and identify new chemotherapeutic agents to achieve more efficient chemotherapy and curing of cancer.

The majority of chemotherapeutic agents are extracted from nature resources and were approved by the United States Food and Drug Administration (USFDA) historically,^{4,5} like paclitaxel, camptothecin and their analogs. Since the late 1980s, a series of natural occurring compounds have attracted great research attentions for their extremely high cytotoxicity.^{6,7} These compounds, to name a few, calicheamicin,⁸ dynemicins,⁹ C-1027,¹⁰ possess the enediyne structure which are readily triggered *in vivo* to generate diradicals through Bergman or Bergman-like cyclization.¹¹ The highly reactive diradicals can abstract the H atoms from the DNA's sugar-phosphate backbones to cause DNA cleavage and finally kill the cancer cells. Much research progress has been made with the natural enediyne antibiotics,¹²⁻¹⁵ and recently the USFDA has approved two antibody drug conjugates, Mylotarg[®] and Besponsa[®], with calicheamicin as the "warhead".^{16,17} Despite their high potential in

developing new anticancer drugs, the enediyne family remains very small because of the limitation on the extraction and total-synthesis technique, with only 11 structurally characterized members known to date¹⁵. Broadening the enediyne family through designing their non-natural analogues is highly important. Many enediyne with various structural features were synthesized and their biological properties were evaluated.¹⁸ In our previous work, we found that the onset temperatures of a thermal Bergman cyclization reaction was drastically lowered when a maleimide moiety was introduced at the ene position.¹⁹ Following this line, we have synthesized several acyclic enediyne antibiotics with maleimide structure to achieve moderate to high cytotoxicity towards tumor cells.²⁰⁻²²

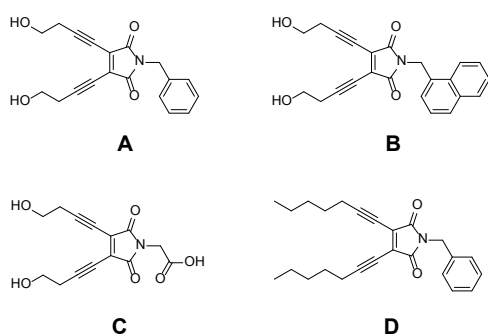
Direct administration of small molecular drugs suffers from low bioavailability, nonspecific cytotoxicity, severe side effects, rapid drug elimination, and severe multidrug resistance (MDR).²³ To this end, nanoscale drug-carriers including liposomes, polymeric micelles, inorganic nano-frameworks have been employed on drug delivery.²⁴⁻²⁸ These nanoscale drug delivery systems show higher therapeutic efficacy and lower side effects than free drugs due to the enhanced permeability and retention (EPR) effect.²⁹ However, the drug-carriers themselves have no therapeutic effect, and the unpredicted degradation of the carriers might cause side-effects.^{30,31} The drug self-delivery systems (DSDSs), in which active drugs exhibit nanoscale characteristic to realize intracellular delivery by themselves have been rapidly developed to address these issues.³²⁻³⁴ The DSDSs hold the following features: (i) accumulation in tumors due to the EPR effect; (ii) excellent drug loading capacities (up to 100% for pure nanodrugs); (iii) no carrier-induced toxicity and immunogenicity.³⁵⁻⁴⁰

This article has been accepted for publication and undergone full peer review but has not been through the copyediting, typesetting, pagination and proofreading process which may lead to differences between this version and the Version of Record. Please cite this article as doi: 10.1002/cjoc.201900034

Herein, we report four maleimide-based enediyne compounds with different hydrophilicity. Among which, two of them exhibit the potential as DSDSs. The two hydroxyl groups endow them hydrophilicity, while the rest parts endow them lipophilicity. When the concentrations of these two enediyne compounds reach the critical aggregation concentration (CAC), self-assembled nanoparticles with size around 100 nm were formed, which would accumulate in tumor tissues through EPR effect and enter the tumor cells by receptor-mediated endocytosis^{41,42}. Encouragingly, the enediyne compounds with DSDS feature show much higher cytotoxicity than their hydrophilic or lipophilic counterparts, suggesting a simple yet efficient drug design strategy.

Results and Discussion

The four enediynes (EDY) (Fig. 1) were synthesized from 3,4-diidomaleimides and terminal alkynes through Sonogashira reaction (ESI). The chemical structure of EDY A-C were verified by ¹H NMR, ¹³C NMR and HR-MS spectroscopies (ESI), while the EDY D is referred to our previous work.⁴³ The molecular structure of the EDY A and B were carefully designed to endow them amphiphilicity to meet the criteria of DSDSs, while the EDY C was designed as a hydrophilic control and EDY D was used as a hydrophobic control. The physicochemical parameters of these enediynes are listed in Table S1. All of the enediyne compounds are likely to exhibit good absorption or permeation to cancer cells according to the Lipinski's Rule of Five (Ro5, MWT ≤ 500, log P ≤ 5, H-bond donors ≤ 5, H-bond acceptors ≤ 10).⁴⁴



1 Chemical structures of enediyne compounds.

The critical aggregation concentration (CAC) of two amphiphilic enediynes were measured by using Nile Red as a fluorescent probe.⁴⁵ The fluorescence emission of Nile Red increases drastically when it is transferred from an aqueous solution to a hydrophobic environment, indicating the formation of micellar (or micelle-like) assembly.⁴⁶⁻⁴⁸ Figure S10 shows that the CAC values of the EDY A and EDY B are 19 μM and 7 μM, respectively. The lower CAC value of EDY B is related to its higher LogP value (Table S1), which is beneficial to promote the formation of self-assembly for DSDSs. The hydrophilic EDY C is freely soluble in aqueous solutions, however, it might encounter difficulty when admitted by tumor cells as cell membranes are lipophilic phospholipid bilayers. The lipophilic EDY D (LogP, 5.46) might enter the tumor cells through penetration or diffusion, but its bioavailability would be rather low due to its low solubility in

cell culturing media or blood stream.

The self-assembled nanoparticles (NPs) of EDY A and B were prepared by slowly adding their THF solutions into water, followed by removal of THF through evaporation. The DLS curves (Figure 2A and 2B) of the assemblies show the formation of EDY NPs with narrow size distributions. The average hydrodynamic diameter of EDY A NPs and EDY B NPs are 97.5 nm and 129 nm, respectively. TEM images (Figure 2C, 2D) show that the NPs are spherical micelles with average diameter of 80 nm for EDY A, and 100 nm for EDY B. The slight difference of the size measured with DLS and TEM is due to the shrinkage of nanoparticles in a drying state during TEM sample preparation.

Enediyne compounds undergo Bergman or Bergman-like cycloaromatization to generate diradical intermediates, endowing them DNA-cleavage ability and cytotoxicity. To verify this transformation, the structural change of the enediyne compounds, in particular, the reaction of the triple bonds was characterized with FT-IR and Raman spectroscopies. EDY A was chosen as the representative compound for this study as all four compounds share the same enediyne core structure. The characteristic peak of the stretching of triple bond in EDY A is observed at 2211 cm⁻¹. This peak disappeared completely after EDY A was kept in methanol at 37°C for 2 days, while the other peaks almost unchanged (Figure S11).

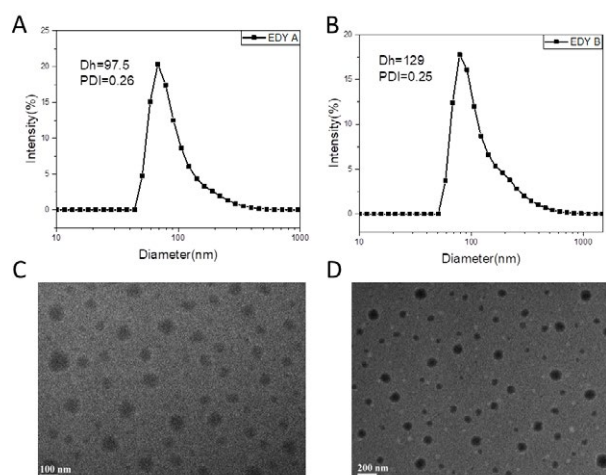


Figure 2 (A) (B) DLS curves of EDY A and EDY B NPs. (C) (D) TEM images of EDY A and EDY B nanoparticles.

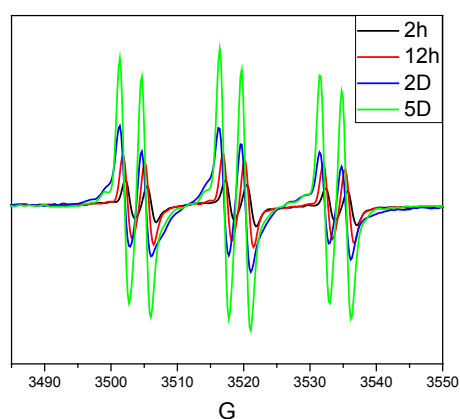
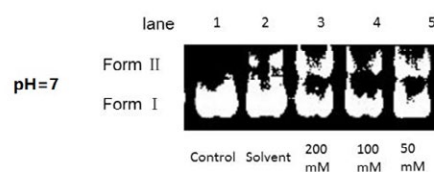


Figure 3 (A) ESR spectra of the EDY A-PBN adduct in methanol at 37 °C.

Electron spin resonance (ESR) spectroscopy analysis was used to verify the radical nature of the cycloaromatization. The highly reactive carbon radicals generated from the reaction were trapped by radical-trapping agents and turn into stable free radicals for ESR study.⁴⁹ Usuki et al. conducted a spin-trapping experiment on calicheamicin to confirm the generation and the evolution of radical species in ethanol solution.⁵⁰ Regarding to this, phenyl tert-butyl nitron (PBN) was used for this experiment (PBN itself shows no ESR signal, Figure S12A). As shown in Figure 3, ESR spectrum of the mixture of EDY A and PBN in methanol exhibits triplet signals⁵¹ with hyperfine coupling of 1.5 mT. The minor triplets in the spectrum might come from the radical species formed from the H-abstraction of the solvent molecules by the highly reactive diradical intermediates followed by radical addition with PBN. Interestingly, the intensity of the recorded ESR signals increased in a time dependent manner in 5 days, suggesting that the generation of radical species from EDY A would last for a long time. Similarly, ESR spectrum of the mixture of EDY B and PBN in DMSO exhibits triplet ESR signals (Figure S12B).

ΦX174 RF1 DNA



PBR322 DNA

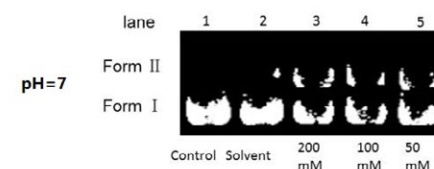


Figure 4 Cleavage of DNA by EDY A at different concentrations for 72 h at 37 °C. Lane 1: DNA (4 μ L) in TE buffer (2 μ L, pH 7.6); lane 2: DNA (4 μ L) + DMSO (2 μ L); Lane 3: DNA (4 μ L) + EDY A (200 mM) in DMSO (2 μ L); lane 4: DNA (4 μ L) + EDY A (100 mM) in DMSO (2 μ L); lane 5: DNA (4 μ L) + EDY A (50 mM) in DMSO (2 μ L)

DNA cleavage experiments were conducted to further prove the ability of the diradicals to abstract H atoms from the DNA's sugar-phosphate backbones. Two kinds of supercoiled plasmid DNA were used for this study by analysing the conversion of DNA from native supercoiled (Form I) to circular relaxed form (Form II, single-strand cleavage).⁶ The supercoiled plasmid DNA was incubated with EDY A at 37 °C for 72 h and then subjected to agarose gel electrophoresis (Figure 4). Free DNA or DNA treated with DMSO were set as control group. The supercoiled DNA are significantly converted to Form II in the presence of EDY A (lane 3, 4, 5) in a concentration dependent manner, while almost no change was found for the control group (lane 1, 2). All the above results indicate that the EDY are able to generate diradical through cycloaromatization at physiological temperature to cause DNA cleavage, endowing them the potential as antitumor agents.

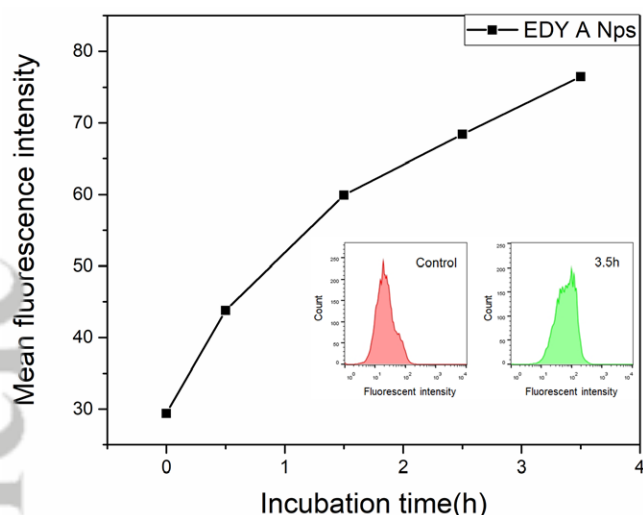


Figure 5 The relative geometrical mean fluorescence intensities of HeLa cells incubated with the EDY A nanoparticles for different time and then analyzed with flow cytometry. Insert: representative flow cytometry histogram profiles of HeLa cells cultured with EDY A nanoparticles for 3.5 h, the untreated cells are used as a control.

It is generally acknowledged that the nanoparticulate drugs with size in the range of tens to hundreds of nanometer could be internalized into cells through receptor-mediated endocytosis⁴¹ while the small molecular drugs mainly go through diffusion. Whether the EDY compounds could be effectively transported into tumor cells is a crucial aspect for their therapeutic efficacy. To this end, confocal laser scanning microscopy (CLSM) and flow cytometry technique were used to evaluate the cellular uptake of the EDY compounds, and HeLa cells were chosen as model cells. Taking advantages of the blue fluorescent emission of these enediyne compounds (Figure S13), they were directly used as the fluorescence probes for the cell internalization analysis.

For CLSM study, HeLa cells were respectively treated with EDY A (5 μ M, below CAC), EDY A NPs (50 μ M, above CAC), EDY C (50 μ M) and cultured for 24 h before observation. Propidium iodide (PI) solution was used to stain the nuclei. As shown in Figure 6a, the small molecular EDY A was found in the cancer cells, proving the successful molecular design of the EDY molecule according to the Lipinski's Rule of Five (Ro5). Interestingly, when the concentration of EDY A is higher than the CAC, both cytoplasm and nuclei of the cells exhibit intense blue fluorescence, demonstrating that EDY A NPs were efficiently internalized by cancer cells in 24 h through endocytosis. The much brighter fluorescence in Figure 6b than that in Figure 6a indicates that the endocytosis of nanoparticulate drugs is more efficient than the diffusion or permeation of the small molecule drugs. In a sharp contrast, even at a high concentration, the blue fluorescence of EDY C is almost invisible in HeLa cells (Fig. 6c), indicating that the highly hydrophilic drug had encountered difficulty to permeate through the lipophilic cytomembrane. Flow cytometry analysis was performed to further confirm the gradual internalization of the EDY A NPs. HeLa cells were firstly incubated with EDY A NPs

(50 μ M) at 37 $^{\circ}$ C for the predetermined time intervals (0.5 h, 1.5 h, 2.5 h and 3.5 h) and then subjected for flow cytometry analysis. The fluorescence of EDY A was monitored with a 375 nm laser and the cells without any treatment were taken as a control. As shown in Figure 5, the fluorescence intensity of EDY A NPs in HeLa cells steadily increases with the extension of culture time.

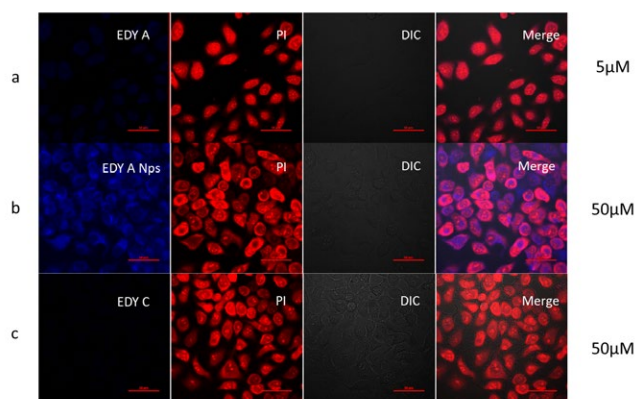


Figure 6 CLSM images of HeLa cells treated with a) EDY A at the concentration of 5 μ M b) EDY A NPs at the concentration of 50 μ M and c) EDY C at the concentration of 50 μ M for 24 h. Cell nuclei are stained with PI. The scale bar represents 50 μ m.

The proliferation inhibition of all four enediyne compounds against a model cancer lines, HeLa cells, was evaluated by 3-(4,5-dimethylthiazol-2-yl)-2,5-diphenyltetrazoliumbromide (MTT) assay. The HeLa cells were firstly cultured with the enediyne compounds at concentrations ranging from 0.9 to 60 μ M and then respectively treated with MTT and characterized with fluorescence spectroscopy. The cells treated with 0.1% DMSO was used as a control. The cell proliferation results are shown in Figure 7. After incubation for 48 h, EDY C almost shows no cytotoxicity within the concentration range, which is in consistent with the cell internalization result. EDY A starts to show the proliferation inhibition of HeLa cells when the concentration is below the CAC value (19 μ M). When the concentration is higher than CAC value, EDY A would self-assemble into nanoparticles and shows profound inhibition of the proliferation of HeLa cells (over 80%). The therapeutic efficacy of EDY B is more dependent on its concentration. When the concentration of EDY B is lower than the CAC value (7 μ M), the cytotoxicity towards HeLa cells is rather low. However, when the concentration of EDY B is higher than the CAC value, the cytotoxicity of the formed EDY B NPs is greatly improved. The IC_{50} concentrations of EDY A (11.2 μ M) and EDY B (10 μ M) are lower than that of their lipophilic analogue EDY D (22.06 μ M) and hydrophilic analogue EDY C (>100 μ M), proving that the DSDSs would greatly enhance the bioavailability of the enediyne compounds and their therapeutic efficiency. Indeed, the cytotoxicity of both EDY A and EDY B are comparable with many clinically used antitumor agents such as doxorubicin and cisplatin.^{52,53}

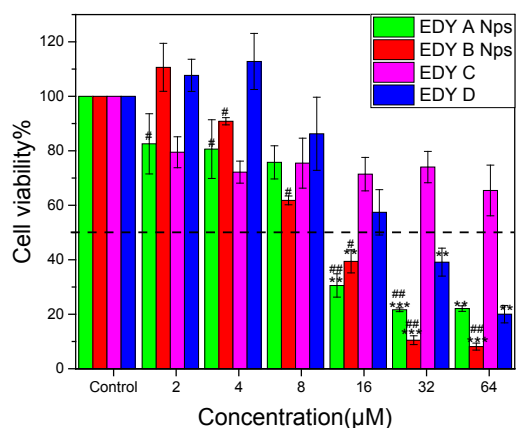


Figure 7 In vitro cytotoxicity study on HeLa cells incubated with different concentrations of EDY A, B Nps and EDY C, D for 24 h determined by MTT assay. Data are shown as means \pm SD ($n = 3$). A significant decrease compared with EDY C-treated cells is denoted by “*” ($P < 0.05$), “**” ($P < 0.01$) and “***” ($P < 0.001$). A significant decrease compared with EDY D-treated cells is denoted by “#” ($P < 0.05$), “##” ($P < 0.01$) and “###” ($P < 0.001$)

Generally, driving tumor cells into apoptosis pathway is a principal mechanism of most cytotoxic drugs to show their chemotherapeutic ability.⁵⁴ To confirm the fact that the induced death of cancer cells incubated with enediynes is mainly through cell apoptosis, fluorescein isothiocyanate (FITC)-Annexin V/PI apoptosis detection kit was applied to qualify the ratio of apoptosis cells. HeLa cells were respectively treated with the enediynes compounds (30 μ M) for 24 h, followed by staining with FITC-Annexin V/PI. The cells without any treatment were applied as a control. As shown in Figure 8, the apoptotic percentages induced by EDY A-D are 64.8%, 86.6%, 20.8%, and 79.4%, respectively, while the necrotic cells were not significant in all groups. The significant higher apoptosis rate induced by the nanoparticulate enediynes compounds (both above their CAC) further corroborate the high efficiency of the amphiphilic DSDSs show great potential in chemotherapy and cancer curing.

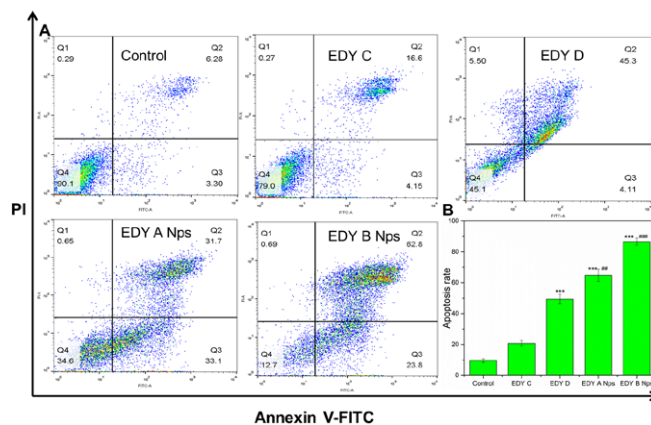


Figure 8 (A) Flow cytometry analysis for apoptosis of HeLa cells induced by EDY A, B Nps and EDY C, D at the concentration of 30 μ M for 24 h. Lower left, living cells; lower right, early apoptotic cells; upper right, late apoptotic cells; upper left, necrotic cells. Inserted numbers in the profiles indicate the percentage of the cells present in this area. (B) Ratio of apoptotic HeLa cells based on the results of flow cytometry measurements. Values represent mean \pm SD ($n = 3$). A significant increase in the apoptosis rate compared with the EDY C-treated cells is denoted with “**” ($P < 0.01$) and “***” ($P < 0.001$), and a significant increase compared with EDY D-treated cells is denoted with “#” ($P < 0.01$) and “###” ($P < 0.001$).

Conclusions

We have designed and synthesized four acyclic enediynes compounds, which are able to generate active diradicals and lead to DNA cleavage through Bergman cyclization or Bergman-like reaction. The molecular amphiphilic nature of two of the enediynes endow them ability to self-assemble into nanoparticles in water and to be self-delivered into tumor tissues through the EPR effect with a high drug loading capacity (100%). After being internalized into the HeLa cells through endocytosis, the self-assembled enediynes nanoparticles would be swallowed by the lysosome and disassembled into free enediynes, which further cause the DNA-cleavage and induce tumor cell death through apoptosis pathway. In comparison, both the hydrophilic and lipophilic enediynes compounds have encountered difficulties to be delivered into tumor cells and resulted in deteriorated cytotoxicity. This study clearly shows that by sophisticated adjusting the hydrophilic/lipophilic balance of a small molecular drug, the therapeutic efficacy could be greatly enhanced, provides a simple yet reasonable guideline for the development of new chemotherapeutic agents with self-delivery feature.

Supporting Information

The supporting information for this article is available on the WWW under <https://doi.org/10.1002/cjoc.2018xxxx>.

Acknowledgement

The financial supports from National Natural Science

Foundation of China (21871080, 21503078, 21474027), the Fundamental Research Funds for the Central Universities (22221818014), and Shanghai Leading Academic Discipline Project (B502) are greatly acknowledged. AH thanks the “Eastern Scholar Professorship” support from Shanghai Local Government. AH thanks Prof. Runhui Liu for his kindly advice in cell experiments.

References

- [1] Bray, F.; Ferlay, J.; Soerjomataram, I.; Siegel, R. L.; Torre, L. A.; Jemal, A. Global cancer statistics 2018: GLOBOCAN estimates of incidence and mortality worldwide for 36 cancers in 185 countries. *CA Cancer J. Clin.* **2018**, *68*, 394-424.
- [2] Torre, L. A.; Bray, F.; Siegel, R. L.; Ferlay, J.; Lortet-Tieulent, J.; Jemal, A. Global cancer statistics, 2012. *CA Cancer J. Clin.* **2015**, *65*, 87-108.
- [3] Xu, Z.; Shi, X.; Hou, M.; Xue, P.; Gao, Y.-E.; Liu, S.; Kang, Y. Disassembly of amphiphilic small molecular prodrug with fluorescence switch induced by pH and folic acid receptors for targeted delivery and controlled release. *Colloids Surf., B* **2017**, *150*, 50-58.
- [4] Qazi, A. K.; Siddiqui, J. A.; Jahan, R.; Chaudhary, S.; Walker, L. A.; Sayed, Z.; Jones, D. T.; Batra, S. K.; Macha, M. A. Emerging therapeutic potential of graviola and its constituents in cancers. *Carcinogenesis* **2018**, *39*, 522-533.
- [5] Newman, D. J. Natural Products as Leads to Potential Drugs: An Old Process or the New Hope for Drug Discovery? *J. Med. Chem.* **2008**, *51*, 2589-2599.
- [6] Kar, M.; Basak, A. Design, Synthesis, and Biological Activity of Unnatural Eneidyne and Related Analogues Equipped with pH-Dependent or Phototriggering Devices. *Chem. Rev.* **2007**, *107*, 2861-2890.
- [7] Zein, N.; Sinha, A. M.; McGahren, W. J.; Ellestad, G. A. Calicheamicin gamma 1: an antitumor antibiotic that cleaves double-stranded DNA site specifically. *Science* **1988**, *240*, 1198-1201.
- [8] Lee, M. D.; Manning, J. K.; Williams, D. R.; Kuck, N. A.; Testa, R. T.; Borders, D. B. Calicheamicins, a novel family of antitumor antibiotics. 3. Isolation, purification and characterization of calicheamicins beta 1Br, gamma 1Br, alpha 2I, alpha 3I, beta 1I, gamma 1I and delta 1I. *J. Antibiot.* **1989**, *42*, 1070-1087.
- [9] Konishi, M.; Ohkuma, H.; Matsumoto, K.; Saitoh, K.; Miyaki, T.; Oki, I.; Kawaguchi, H. Dynemicins, new antibiotics with the 1, 5-diyne-3-ene and anthraquinone subunit. I. Productin, isolation and physico-chemical properties. *J. Antibiot.* **1991**, *44*, 1300-1305.
- [10] Hirama, M.; Akiyama, K.; Tanaka, T.; Noda, T.; Iida, K.-i.; Sato, I.; Hanaishi, R.; Fukuda-Ishisaka, S.; Ishiguro, M.; Otani, T.; Leet, J. E. Paramagnetic Eneidyne Antibiotic C-1027: Spin Identification and Characterization of Radical Species. *J. Am. Chem. Soc.* **2000**, *122*, 720-721.
- [11] Nicolaou, K. C.; Sorensen, E. J.; Discordia, R.; Hwang, C.-K.; Bergman, R. G.; Minto, R. E.; Bharucha, K. N. Ten-Membered Ring Eneidyne with Remarkable Chemical and Biological Profiles. *Angew. Chem. Int. Ed. Eng.* **1992**, *31*, 1044-1046.
- [12] Wang, R.; Li, L.; Zhang, S.; Li, Y.; Wang, X.; Miao, Q.; Zhen, Y. A novel enediyne - integrated antibody - drug conjugate shows promising antitumor efficacy against CD30+ lymphomas. *Mol. Oncol.* **2018**, *12*, 339-355.
- [13] Chang, C.-Y.; Yan, X.; Crnovcic, I.; Annava, T.; Chang, C.; Nocek, B.; Rudolf, J. D.; Yang, D.; Hindra; Babnigg, G.; Joachimiak, A.; Phillips, G. N.; Shen, B. Resistance to Eneidyne Antitumor Antibiotics by Sequestration. *Cell Chem. Biol.* **2018**, *25*, 1075-+.
- [14] Li, L.; Hu, L.; Zhao, C.-y.; Zhang, S.-h.; Wang, R.; Li, Y.; Shao, R.-g.; Zhen, Y.-s. The Recombinant and Reconstituted Novel Albumin-Lidamycin Conjugate Shows Lasting Tumor Imaging and Intensively Enhanced Therapeutic Efficacy. *Bioconjugate Chem.* **2018**, *29*, 3104-3112.
- [15] Yan, X. H.; Ge, H. M.; Huang, T. T.; Hindra; Yang, D.; Teng, Q. H.; Crnovcic, I.; Li, X. L.; Rudolf, J. D.; Lohman, J. R.; Gansemans, Y.; Zhu, X. C.; Huang, Y.; Zhao, L. X.; Jiang, Y.; Van Nieuwerburgh, F.; Rader, C.; Duan, Y. W.; Shen, B. Strain Prioritization and Genome Mining for Eneidyne Natural Products. *Mbio* **2016**, *7*.
- [16] Thomas, A.; Teicher, B. A.; Hassan, R. Antibody-drug conjugates for cancer therapy. *Lancet Oncol.* **2016**, *17*, e254-e262.
- [17] Bross, P. F.; Beitz, J.; Chen, G.; Chen, X. H.; Duffy, E.; Kieffer, L.; Roy, S.; Sridhara, R.; Rahman, A.; Williams, G.; Pazdur, R. Approval Summary: Gemtuzumab Ozogamicin in Relapsed Acute Myeloid Leukemia. *Clin. Cancer Res.* **2001**, *7*, 1490-1496.
- [18] Romeo, R.; Giofre, S. V.; Chiacchio, M. A. Synthesis and Biological Activity of Unnatural Eneidyne. *Curr. Med. Chem.* **2017**, *24*, 3433-3484.
- [19] Sun, S.; Zhu, C.; Song, D.; Li, F.; Hu, A. Preparation of conjugated polyphenylenes from maleimide-based enediynes through thermal-triggered Bergman cyclization polymerization. *Polym. Chem.* **2014**, *5*, 1241-1247.
- [20] Song, D.; Tian, Y.; Huang, S.; Li, B.; Yuan, Y.; Hu, A. An acyclic enediyne with a furyl tethering group for efficient inhibition of tumor cell viability. *J. Mater. Chem. B* **2015**, *3*, 8584-8588.
- [21] Song, D.; Sun, S.; Tian, Y.; Huang, S.; Ding, Y.; Yuan, Y.; Hu, A. Maleimide-based acyclic enediyne for efficient DNA-cleavage and tumor cell suppression. *J. Mater. Chem. B* **2015**, *3*, 3195-3200.
- [22] Li, J.; Li, B.; Sun, L.; Duan, B.; Huang, S.; Yuan, Y.; Ding, Y.; Hu, A. Self-delivery nanoparticles of an amphiphilic irinotecan-enediynes conjugate for cancer combination chemotherapy. *J. Mater. Chem. B* **2019**, *7*, 103-111.
- [23] Huttunen, K. M.; Raunio, H.; Rautio, J. Prodrugs—from Serendipity to Rational Design. *Pharmacol. Rev.* **2011**, *63*, 750-771.
- [24] Tarn, D.; Ashley, C. E.; Xue, M.; Carnes, E. C.; Zink, J. I.; Brinker, C. J. Mesoporous Silica Nanoparticle Nanocarriers: Biofunctionality and Biocompatibility. *Acc. Chem. Res.* **2013**, *46*, 792-801.
- [25] Zhang, J.; Yuan, Z.-F.; Wang, Y.; Chen, W.-H.; Luo, G.-F.; Cheng, S.-X.; Zhuo, R.-X.; Zhang, X.-Z. Multifunctional Envelope-Type Mesoporous Silica Nanoparticles for Tumor-Triggered Targeting Drug Delivery. *J. Am. Chem. Soc.* **2013**, *135*, 5068-5073.
- [26] Wang, W.; Despanie, J.; Shi, P.; Edman, M. C.; Lin, Y.-A.; Cui, H.; Heur, M.; Fini, M. E.; Hamm-Alvarez, S. F.; MacKay, J. A. Lacritin-mediated regeneration of the corneal epithelia by protein polymer nanoparticles. *J. Mater. Chem. B* **2014**, *2*, 8131-8141.
- [27] Sun, T.; Zhang, Y. S.; Pang, B.; Hyun, D. C.; Yang, M.; Xia, Y. Engineered Nanoparticles for Drug Delivery in Cancer Therapy. *Angew. Chem. Int. Ed.* **2014**, *53*, 12320-12364.
- [28] Hubbell, J. A.; Chilkoti, A. Nanomaterials for Drug Delivery. *Science* **2012**, *337*, 303-305.
- [29] Maeda, H. Toward a full understanding of the EPR effect in primary

- and metastatic tumors as well as issues related to its heterogeneity. *Adv. Drug Del. Rev.* **2015**, *91*, 3-6.
- [30] Yu, D.; Peng, P.; Dharap, S. S.; Wang, Y.; Mehlig, M.; Chandna, P.; Zhao, H.; Filpula, D.; Yang, K.; Borowski, V.; Borchard, G.; Zhang, Z.; Minko, T. Antitumor activity of poly(ethylene glycol)-camptothecin conjugate: The inhibition of tumor growth in vivo. *J. Controlled Release* **2005**, *110*, 90-102.
- [31] Greenwald, R. B.; Choe, Y. H.; McGuire, J.; Conover, C. D. Effective drug delivery by PEGylated drug conjugates. *Adv. Drug Del. Rev.* **2003**, *55*, 217-250.
- [32] He, D.; Zhang, W.; Deng, H.; Huo, S.; Wang, Y.-F.; Gong, N.; Deng, L.; Liang, X.-J.; Dong, A. Self-assembling nanowires of an amphiphilic camptothecin prodrug derived from homologous derivative conjugation. *Chem. Commun.* **2016**, *52*, 14145-14148.
- [33] Fumagalli, G.; Marucci, C.; Christodoulou, M. S.; Stella, B.; Dosio, F.; Passarella, D. Self-assembly drug conjugates for anticancer treatment. *Drug Discov. Today* **2016**, *21*, 1321-1329.
- [34] Duan, X.; Chen, H.; Fan, L.; Kong, J. Drug Self-Assembled Delivery System with Dual Responsiveness for Cancer Chemotherapy. *ACS Biomater. Sci. Eng.* **2016**, *2*, 2347-2354.
- [35] Qin, S.-Y.; Zhang, A.-Q.; Cheng, S.-X.; Rong, L.; Zhang, X.-Z. Drug self-delivery systems for cancer therapy. *Biomaterials* **2017**, *112*, 234-247.
- [36] Wang, Y.; Huang, P.; Hu, M.; Huang, W.; Zhu, X.; Yan, D. Self-Delivery Nanoparticles of Amphiphilic Methotrexate-Gemcitabine Prodrug for Synergistic Combination Chemotherapy via Effect of Deoxyribonucleotide Pools. *Bioconjugate Chem.* **2016**, *27*, 2722-2733.
- [37] Mou, Q.; Ma, Y.; Zhu, X.; Yan, D. A small molecule nanodrug consisting of amphiphilic targeting ligand-chemotherapy drug conjugate for targeted cancer therapy. *J. Controlled Release* **2016**, *230*, 34-44.
- [38] Huang, P.; Ao, J.; Zhou, L.; Su, Y.; Huang, W.; Zhu, X.; Yan, D. Facile Approach To Construct Ternary Cocktail Nanoparticles for Cancer Combination Therapy. *Bioconjugate Chem.* **2016**, *27*, 1564-1568.
- [39] Zhang, T.; Huang, P.; Shi, L.; Su, Y.; Zhou, L.; Zhu, X.; Yan, D. Self-Assembled Nanoparticles of Amphiphilic Twin Drug from Floxuridine and Bendamustine for Cancer Therapy. *Mol. Pharmaceutics* **2015**, *12*, 2328-2336.
- [40] Huang, P.; Wang, D.; Su, Y.; Huang, W.; Zhou, Y.; Cui, D.; Zhu, X.; Yan, D. Combination of small molecule prodrug and nanodrug delivery: amphiphilic drug-drug conjugate for cancer therapy. *J. Am. Chem. Soc.* **2014**, *136*, 11748-11756.
- [41] Gao, H. J.; Shi, W. D.; Freund, L. B. Mechanics of receptor-mediated endocytosis. *Proc. Natl. Acad. Sci. U. S. A.* **2005**, *102*, 9469-9474.
- [42] Bareford, L. A.; Swaan, P. W. Endocytic mechanisms for targeted drug delivery. *Adv. Drug Del. Rev.* **2007**, *59*, 748-758.
- [43] Huang, S.; Li, J.; Li, B.; Hu, A. Design, synthesis and cytotoxicity study of a novel acyclic enediyne. *J. East Chin. Univ. Sci. & Tech.* **2017**, *43*, 1-7.
- [44] Lipinski, C. A. Lead- and drug-like compounds: the rule-of-five revolution. *Drug Discovery Today: Technol.* **2004**, *1*, 337-341.
- [45] Shen, Y.; Jin, E.; Zhang, B.; Murphy, C. J.; Sui, M.; Zhao, J.; Wang, J.; Tang, J.; Fan, M.; Van Kirk, E.; Murdoch, W. J. Prodrugs Forming High Drug Loading Multifunctional Nanocapsules for Intracellular Cancer Drug Delivery. *J. Am. Chem. Soc.* **2010**, *132*, 4259-4265.
- [46] Shi, C.; Guo, D.; Xiao, K.; Wang, X.; Wang, L.; Luo, J. A drug-specific nanocarrier design for efficient anticancer therapy. *Nature Commun.* **2015**, *6*, 7449.
- [47] Harnoy, A. J.; Rosenbaum, I.; Tirosh, E.; Ebenstein, Y.; Shaharabani, R.; Beck, R.; Amir, R. J. Enzyme-Responsive Amphiphilic PEG-Dendron Hybrids and Their Assembly into Smart Micellar Nanocarriers. *J. Am. Chem. Soc.* **2014**, *136*, 7531-7534.
- [48] Edwardson, T. G. W.; Carneiro, K. M. M.; McLaughlin, C. K.; Serpell, C. J.; Sleiman, H. F. Site-specific positioning of dendritic alkyl chains on DNA cages enables their geometry-dependent self-assembly. *Nature Chem.* **2013**, *5*, 868.
- [49] Mifsud, N.; Mellon, V.; Perera, K. P. U.; Smith, D. W.; Echegoyen, L. In situ EPR spectroscopy of aromatic diene cyclopolymerization. *J. Org. Chem.* **2004**, *69*, 6124-6127.
- [50] Usuki, T.; Kawai, M.; Nakanishi, K.; Ellestad, G. A. Calicheamicin gamma(l)(1) and phenyl tert-butyl nitron (PBN): observation of a kinetic isotope effect by an ESR study. *Chem. Commun.* **2010**, *46*, 737-739.
- [51] Luckhurst, G. R. Alternating linewidths. A novel relaxation process in the electron resonance of biradicals. *Mol. Phys.* **1966**, *10*, 543-550.
- [52] Dhar, S.; Lippard, S. J. Mitaplatin, a potent fusion of cisplatin and the orphan drug dichloroacetate. *Proc. Natl. Acad. Sci.* **2009**, *106*, 22199-22204.
- [53] He, H. Y.; Zhao, J. N.; Jia, R.; Zhao, Y. L.; Yang, S. Y.; Yu, L. T.; Yang, L. Novel Pyrazolo[3,4-d] pyrimidine Derivatives as Potential Antitumor Agents: Exploratory Synthesis, Preliminary Structure-Activity Relationships, and in Vitro Biological Evaluation. *Molecules* **2011**, *16*, 10685-10694.
- [54] Hengartner, M. O. The biochemistry of apoptosis. *Nature* **2000**, *407*, 770.

(The following will be filled in by the editorial staff)

Manuscript received: XXXX, 2019

Manuscript revised: XXXX, 2019

Manuscript accepted: XXXX, 2019

Accepted manuscript online: XXXX, 2019

Version of record online: XXXX, 2019

Entry for the Table of Contents

Page No.

Self-delivery nanoparticles of amphiphilic acyclic enediynes for efficient tumor cell suppression

g Li, Yuequn Wu, Lili Sun, Shuai Huang, Baojun Li, Yun Ding, Aiguo Hu*

↕ Max. Table height 6 cm ↕

